JOURNAL OF Materials CHEMISTRY

Synthesis and characterization of ordered mesoporous silicas with high loadings of methyl groups

Michal Kruk,[a] Tewodros Asefa,[b] Neil Coombs,[b] Mietek Jaroniec*[a] and Geoffrey A. Ozin*[b]

[a]*Department of Chemistry, Kent State University, Kent, OH 44240, USA. E-mail: Jaroniec@columbo.kent.edu*
[b]*Materials Chemistry Research Group, Department of Chemistry, University of Toronto, 80 St. George Street, Toronto, Ontario, Canada M5S 3H6. E-mail: gozin@chem.utoronto.ca*

Received 29th May 2002, Accepted 4th September 2002
First published as an Advance Article on the web 4th October 2002

Ordered silicas with high loadings of pendant methyl groups were synthesized *via* cocondensation of tetraethyl orthosilicate and triethoxymethylsilane under basic conditions in the presence of cetyltrimethylammonium surfactant. The resulting materials were characterized using X-ray diffraction (XRD), transmission electron microscopy (TEM), ^{29}Si and ^{13}C NMR spectroscopy, nitrogen adsorption and thermogravimetry. For lower loadings of the organosilane in the synthesis mixture, XRD patterns were characteristic of a 2-dimensional hexagonal structure. As seen from XRD, the degree of structural ordering diminished as the loading increased, but an XRD pattern with a single pronounced peak and TEM images characteristic of a 2-dimensional hexagonal structure were recorded even for a methyl-functionalized silica with about 50% of silicon atoms carrying the organic groups. The extent of organosilane incorporation was found to be nearly quantitative. The methyl groups were stable during surfactant removal, both *via* solvent extraction and pyrolysis at 573 K under nitrogen. The (100) interplanar spacing and the pore diameter were found to decrease from 3.45 to 3.12 nm, and from 2.9 to 2.3 nm, respectively, as the loading of the organosilane increased up to 43%, but no further decrease was observed when the loading increased to 50%. The BET specific surface area was relatively constant (720–800 $m^2\ g^{-1}$) for loadings of 20–50%, whereas the primary pore volume decreased as the loading of organics increased. Nitrogen adsorption provided some evidence of phase separation into organosilicate-rich and silicate-rich phases for methyl group loadings of 33% or higher and particularly for the 50% loading. Thermogravimetric data suggested that the methyl groups are highly thermally stable in both nitrogen and air atmospheres.

Introduction

The discovery of ordered mesoporous silicas[1,2] in the early nineties opened remarkably broad opportunities in the synthesis of ordered mesoporous organic–inorganic composites.[3,4] The latter include materials with silica frameworks and organic groups on the pore surface,[1,5–7] and materials with organosilica frameworks,[8–13] whose pore surface can be covered by organic groups.[12,13] Organic-functionalized ordered mesoporous silicas can be synthesized using several methods, such as: (i) post-synthesis functionalization of surfactant-free silicas;[1,14,15] (ii) post-synthesis functionalization of surfactant-containing materials involving surfactant-displacement reactions;[5,16–18] (iii) direct synthesis *via* cocondensation of organosilica and silica precursors;[6,7] and (iv) thermally induced transformation of organosilicas with hybrid organic–inorganic frameworks to silicas with pendent organic groups.[11] Among the methods for the synthesis of ordered silicas with surface organic functionality, the direct synthesis *via* cocondensation is particularly attractive from a practical point of view, because it is simple, efficient,[3,4,19] and it allows one to achieve the highest loadings of organic groups.[20–22] In fact, more than 60% of the silicon atoms can carry pendent organic groups in ordered materials synthesized *via* cocondensation.[21,22]

Methyl is the smallest organic group that can be introduced on the surface of silica-based material using the cocondensation method. Although methyl groups bonded to the silica surface are chemically inert and do not exhibit any useful adsorption or catalytic properties by themselves, their presence introduces hydrophobic properties,[23–30] and leads to improved hydrothermal[29] as well as mechanical stabilities.[29,30] Consequently, a cocondensation method was used to synthesize (i) highly active titanosilicate epoxidation catalysts with surface methyl groups,[23–25] or both methyl and 3-chloropropyl groups,[28] (ii) a catalyst with both sulfonic acid and methyl groups that was active in esterification reactions,[26,27] and (iii) a catalyst with both methyl and aminopropyl groups that was active in the Knoevenagel reaction.[19] These catalysts were synthesized under neutral conditions in the presence of neutral amines[19] or under basic conditions in the presence of cationic surfactants.[23–28] The cocondensation synthesis of methyl-functionalized silicas under acidic conditions,[30,31] and the synthesis of a silica with both methyl and ureidopropyl groups under neutral conditions using an oligomeric surfactant[32] were also studied. Similarly to typical results presented on cocondensation syntheses of silicas with other organic groups,[33–39] methyl-functionalized silicas were well ordered when 35% or less of silicon atoms were decorated by methyl groups, although some residual ordering was observed even when 50% functionalization was attempted[23] based on the synthesis gel composition. However, for the latter, no data was reported that would allow one to assess the actual functionalization level.

Very recently, we have reported a successful cocondensation synthesis of silicas with unprecedented loadings of pendent vinyl groups.[21,22] Up to 62% of silicon atoms were functionalized with vinyl groups in ordered materials. Even slightly higher organic functionalization was attained with retention of the ordered structure, but for the latter, there was some evidence for the occurrence of separation into a disordered organosilicate-rich and an ordered silicate-rich phases. We

 DOI: 10.1039/b205217b

have mentioned that the same synthesis procedure allows one to synthesize ordered methyl-functionalized silicas with up to about 50% loading of organic groups (which is higher than any loading documented in the literature for these materials), but there is some evidence of phase separation for loadings of 33–50%. Herein, the structural and surface properties of ordered methyl-functionalized materials with loadings of 20–50%, as well as disordered high-surface-area 100% methylsilica, are reported. The evidence of phase separation for 33–50% loadings is presented, along with evidence for a quantitative incorporation of the organosilica precursor for material with 50% methyl group loading. In addition, methods for surfactant removal and the high thermal stability of the methyl-functionalized materials are discussed.

Experimental

Synthesis

Methyl-functionalized silicas were synthesized as described elsewhere[21,22] using the following synthesis gel composition: x/100 TEMS : (100 − x)/100 TEOS : 0.24 CTAB : 16.10 NH_4OH : 128.70 H_2O, where CTAB, TEMS, and TEOS denote cetyltrimethylammonium bromide, triethoxymethylsilane, and tetraethyl orthosilicate, respectively. CTAB, TEOS and TEMS were obtained from Aldrich and were used as received. The amount of organosilane was varied from $x = 20$ to 100. The typical synthesis procedure was as follows. A solution of CTAB (0.54 g, 1.48 mmol), NH_4OH (5.7 g, 30 wt.%, 0.10 mol) and water (10.6 g, 0.59 mol) was prepared at room temperature in a tightly closed plastic bottle. To this solution was added 6.23 mmol of the silica source prepared from a mixture of TEOS and TEMS. The mixture was stirred for 30 min at room temperature and subsequently aged at 353 K for 4 days. Then, the product was filtered, washed thoroughly with large amounts of water and dried under ambient atmosphere to obtain a fine white powder. The surfactant was extracted from the as-synthesized materials by mildly stirring *ca.* 0.2 g of the sample in HCl (5 g, 35 wt.%)/methanol (100 g) solution at 313 K for 6 h. Subsequently, the product was filtered on a Büchner funnel, washed with methanol, and dried in air. Alternatively, the surfactant was removed by calcining the as-synthesized samples at 573 K under a flow of nitrogen for *ca.* 3.5 h in a temperature programmable furnace after raising the temperature from room temperature to 573 over a 1 h period while the sample is inside the furnace. The sample prepared from 100% TEMS was a gel after aging for 4 days and therefore the bottle was left open at 353 K to let the solvent evaporate and to obtain a solid product. The resulting samples are referred to as MExA, and MExE, where x reflects the synthesis gel composition, and A and E denote samples in as-synthesized or solvent-extracted forms, respectively.

Characterization

Powder XRD patterns were recorded on a Siemens D5000 diffractometer operating at 35 mA/50 kV using Ni-filtered Cu Kα radiation. Solid state ^{13}C (100.6 MHz) and ^{29}Si (79.5 MHz) NMR spectra were acquired on a Bruker DSX 400 spectrometer with the following experimental parameters: for ^{13}C CP-MAS NMR experiments, 6.5 kHz spin rate, 3 s recycle delay, 2 ms contact time, $\pi/2$ pulse width of 6.5 μs, 5,000–10,000 scans; for ^{29}Si CP-MAS NMR experiments, 6.5 kHz spin rate, 3 s recycle delay, 10 ms contact time, $\pi/2$ pulse width of 6.0–7.5 μs, 200–1,000 scans; and for ^{29}Si MAS NMR experiments, 6.5 kHz spin rate, 100 s recycle delay, $\pi/6$ pulse width of 2.2 μs, 500–1,000 scans were used. Adamantane (major peak, 38.4 ppm *vs.* TMS) and $Si[Si(CH_3)_3]_4$ (major peak, −9.98 ppm *vs.* TMS) were used as external references for ^{13}C and ^{29}Si spectra, respectively. Nitrogen adsorption measurements were carried out at 77 K on a Micromeritics ASAP 2010 volumetric adsorption analyzer. Before the measurements, the samples were outgassed at 413 or 573 K under vacuum in a degassing port of the adsorption analyzer for 2 h or until the residual pressure was equal to or below 6 μm Hg. The weight change curves under nitrogen and air atmospheres were recorded on a TA Instruments TGA 2950 thermogravimetric analyzer in a high-resolution mode with a maximum heating rate of 5 K min^{-1}.

The BET specific surface area[40] was evaluated from nitrogen adsorption data in a relative pressure range from 0.01 to 0.02. The latter range was shown elsewhere to be suitable for the estimation of the specific surface area for small-pore silicas.[41] The total pore volume[40] was estimated from the amount adsorbed at a relative pressure of 0.99. The primary (ordered) mesopore volume and the external surface area were calculated using the α_s plot method[40,42] in the α_s range from 1.5 to 2.0 (α_s is defined as the amount adsorbed at a given relative pressure divided by the amount adsorbed at a relative pressure of 0.4). A reference adsorption isotherm for a macroporous silica[42] was used in the α_s plot analysis. The pore size distribution (PSD) was calculated using the Barrett–Joyner–Halenda (BJH) algorithm[43] with the pore diameter–capillary condensation pressure relation[44] and the statistical film thickness curve[42,44] determined using a series of MCM-41 silicas with a wide range of pore sizes. The mesopore diameter is defined as a position of the maximum on the PSD.

Results and discussion

As can be seen in Fig. 1, as-synthesized methyl-functionalized silicas exhibited at least one XRD peak for TEMS : TEOS molar ratios up to 1 : 1 in the synthesis mixture (up to the intended organic functionalization level of 50%), whereas the XRD pattern for the sample prepared from pure TEMS under the same conditions was featureless. It should be noted that the synthesis of samples with methyl group loadings of between 50 and 100% was not attempted, because there was evidence that the sample at 50% functionalization level exhibited some phase separation (see below). Samples with methyl group loadings of 20 and 33% exhibited two additional weaker XRD peaks that can be indexed as (110) and (200) for the 2-D hexagonal structure. The ordered materials retained their ordering after solvent extraction of the surfactant (see Fig. 2). As the loading of TEMS in the synthesis mixture increased from 20 to 43%, the position of the main XRD reflection shifted to higher angles (see Figs. 1 and 2), which corresponded to the (100) interplanar spacing decrease from 3.45 to 3.12 nm for solvent-extracted samples (see Fig. 3 and Table 1). No further lowering of the interplanar spacing was observed when the loading was increased to 50%. The (100) interplanar spacings for solvent-extracted samples tended to be slightly lower than those for as-synthesized samples.

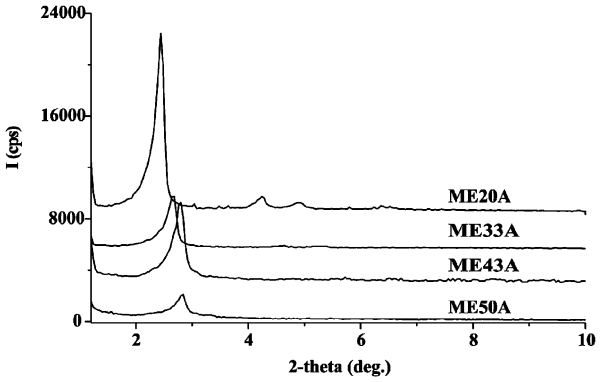

Fig. 1 XRD patterns for as-synthesized methyl-functionalized silicas.

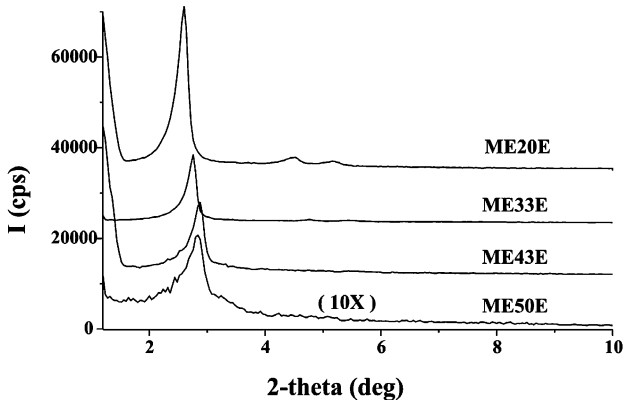

Fig. 2 XRD patterns for solvent-extracted methyl-functionalized silicas.

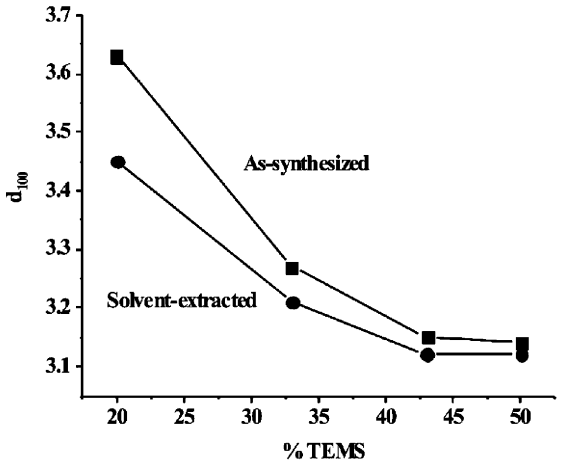

Fig. 3 (100) Interplanar spacing as a function of the TEMS loading in the synthesis mixture.

The ordered structure of the materials was further corroborated by transmission electron microscopy (TEM). Shown in Fig. 4 are TEM images for ME50E that are identified as (A) a projection through the channels and (B) a side view of the channels of a 2-D hexagonal structure. It is interesting to note that on the basis of XRD patterns, this sample was the least ordered among the ordered methyl-functionalized materials, but anyway its TEM images clearly showed arrays of 2-D hexagonally ordered pores.

The ^{29}Si MAS NMR spectrum was acquired for the solvent-extracted ordered ME50E material with the highest intended methyl group loading (see Fig. 5). Resonances corresponding to Q_4, Q_3, T_3, T_2 sites at -111, -101, -65, -55, respectively, as well as a small peak corresponding to Q_2 at -91 ppm were observed. These peak position assignments correspond with similar silicon sites in pure MCM-41 materials and

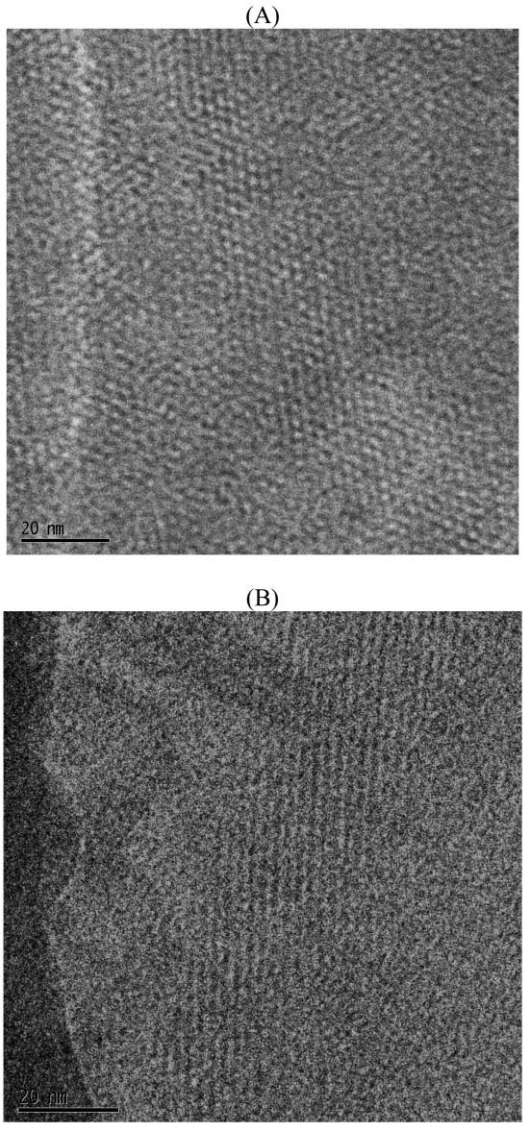

Fig. 4 TEM images of ME50E sample.

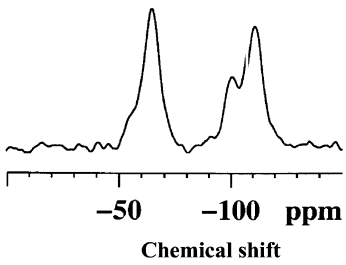

Fig. 5 ^{29}Si MAS NMR spectrum for solvent-extracted methyl-functionalized silica with 50% loading of TEMS in the synthesis mixture.

Table 1 Structural properties[a] of methyl-functionalized silicas

Sample	d_{100}/nm	S_{BET}/m^2 g^{-1}	V_t/cm^3 g^{-1}	V_p/cm^3 g^{-1}	S_{ex}/m^2 g^{-1}	w/nm	b/nm
ME20E	3.45	800	0.70	0.65	20	2.9	1.1
ME33E	3.20	720	0.64	0.50	70	2.6	1.1
ME43E	3.12	740	0.55	0.42	110	2.3	1.3
ME50E	3.12	760	0.73	0.38	280	2.4	1.2
ME100E	—[b]	580	1.61	0.00	—[c]	—[d]	—[e]

[a] d_{100}, (100) interplanar spacing; S_{BET}, BET specific surface area; V_t, total pore volume; V_p, primary mesopore volume; S_{ex}, external surface area; w, pore diameter; b, pore wall thickness. [b] No XRD peaks observed. [c] S_{BET} can be considered as S_{ex}. [d] No observable peak for primary pores on pore size distribution. [e] It was not possible to determine the pore wall thickness for this sample because of its disordered structure, see also footnotes *b* and *d*.

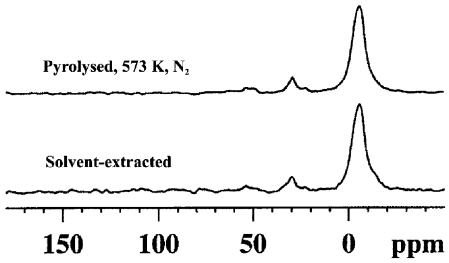

Fig. 6 ^{13}C CP MAS NMR spectrum for solvent-extracted and pyrolysed methyl-functionalized silica with 50% loading of methylsilica precursor in the synthesis mixture.

organosilicates containing *Si*–C(sp^3) silicon sites.[1,11] Furthermore, the material made from 100% TEMS showed only a peak at −65 ppm corresponding exclusively to T_3, which is common to materials made from pure organotrialkoxysilanes.[12] Herein, a standard NMR notation is adopted in which Q_n sites are silicon atoms connected with *n* other silicon atoms *via* oxygen bridges and with $4 - n$ silanols (–OH groups), whereas T_n sites are silicon atoms connected with one organic group *via* Si–C bond, with *n* silicon atoms *via* oxygen bridges and with $3 - n$ silanols. On the basis of the ^{29}Si MAS NMR data, the formula of the ME50E sample was established as $SiO_{1.60}(OH)_{0.34}(CH_3)_{0.46}$ (this formula neglects the presence of residual surfactant), which shows that 46% of silicon atoms are decorated with methyl groups. The value is quite close to the theoretical 50% based on the synthesis mixture composition, and thus shows that a nearly stoichiometric incorporation of TEMS in the structure was observed for this ordered methyl-functionalized silica with a very high methyl group loading. ^{13}C CP MAS NMR spectra (Fig. 6) showed that methyl groups were intact in the solvent-extracted ME50E sample. The methyl groups also survived during pyrolysis of the as-synthesized (surfactant-containing) material at 573 K under nitrogen, which led to the complete removal of the surfactant. The elemental analysis of the pyrolysed ME50 material showed 8.22 wt.% C, 2.46 wt.% H, <0.05 wt.% N, and 43.44 wt.% Si. This indicates a molar ratio of 0.44 C : 1.58 H : <0.002 N : 1 Si, which is consistent with the composition of the surfactant extracted materials that shows a Si : C ratio of 1 : 0.46 (see above). Moreover, it is clear from the wt.% N that the surfactant was essentially completely removed during the pyrolysis. Therefore, surfactant removal for methyl-functionalized silicas can be achieved by using either solvent extraction, or pyrolysis at an appropriate temperature under nitrogen. The content of surfactant in as-synthesized methyl-functionalized materials decreased as the loading of TEMS increased (compare the weight losses centered at about 500 K in Fig. 7), which is similar to the behavior of vinyl-functionalized silicas that were recently described in detail.[21,22] The content of surfactant after solvent extraction was 2–5% based on TGA data (Fig. 8). Interestingly, the surfactant residue for the vinyl-functionalized materials prepared and extracted under the same conditions was usually found to be below 2%. Methyl groups decomposed at temperatures about 800 K under air (see Fig. 8), consistent with an earlier study,[26] and their decomposition extended to about 1000 K under nitrogen. Clearly, methyl groups were more thermally stable than vinyl groups under both nitrogen and air atmospheres, which is also consistent with previous reports.[11,12]

Nitrogen adsorption isotherms for the samples prepared with 20–50% TEMS loading in the synthesis mixture are shown in Fig. 9. The shape of the adsorption isotherm gradually changed from type IV to type I[40,45] as the content of the organic

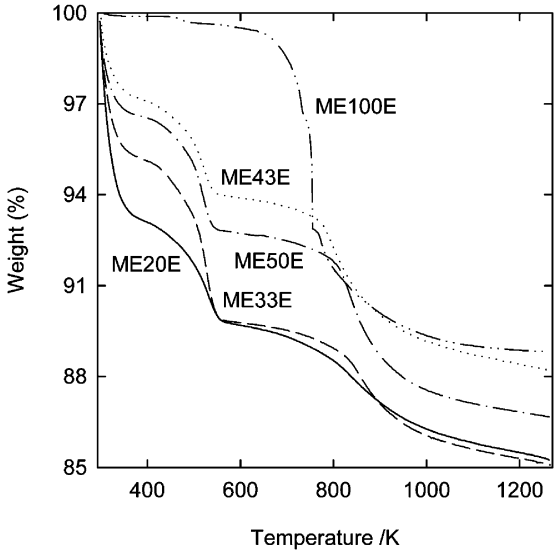

Fig. 8 Weight change curves under air atmosphere for methyl-functionalized silicas.

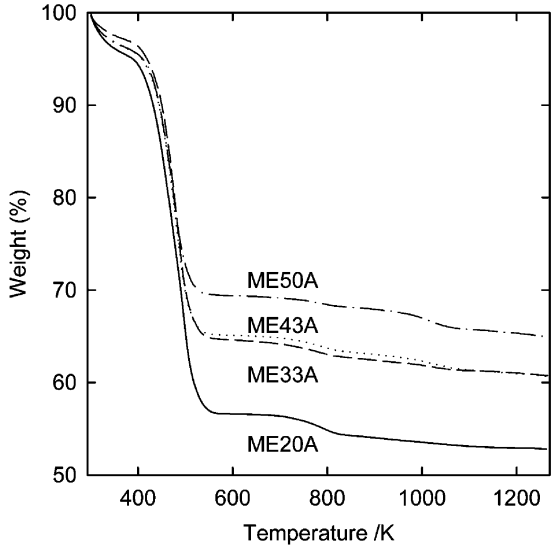

Fig. 7 Weight change curves under nitrogen atmosphere for as-synthesized methyl-functionalized silicas.

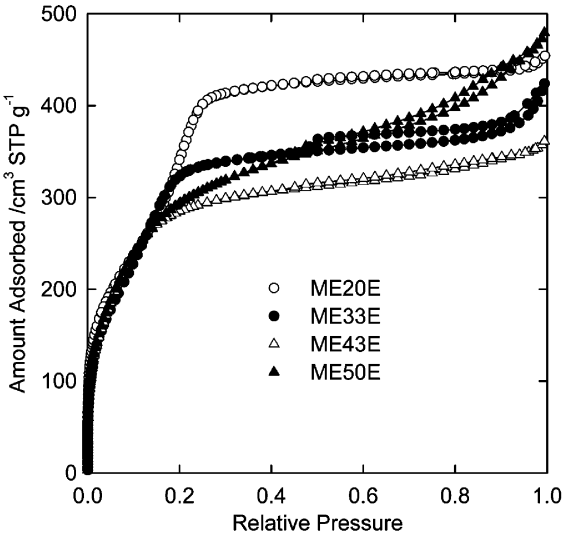

Fig. 9 Nitrogen adsorption isotherms for methyl-functionalized silicas with 20–50% loadings of methyl groups.

groups increased. Type IV isotherms are characteristic of mesoporous materials (pore diameters from 2 to 50 nm) and exhibit pronounced capillary condensation/evaporation steps (which coincide below the lower limit of adsorption–desorption hysteresis, but do not coincide at pressures above this limit, thus leading to a hysteresis). The type I adsorption isotherms level off at quite low relative pressures (when shown in the linear pressure scale) and are observed for microporous materials (pore diameter below 2 nm) and mesoporous materials with pore size close to the micropore range. Thus, the observed change in the adsorption isotherm type as the organic group loading increased is indicative of the decrease in pore diameter. As can be seen in Fig. 10, the pore diameter decrease from 2.9 to 2.3 nm took place as the organic group loading increased from 20 to 43%, whereas a further increase in the loading to 50% did not produce any further pore diameter diminution. These changes in the pore diameter paralleled the change in the (100) interplanar spacing (see Table 1). The increase in the methyl group loading in the synthesis mixture from 20 to 43% led to the primary pore volume decrease, and the external surface area increase, whereas the BET specific surface area was largely unchanged (see Table 1 and Fig. 10). The pore wall thickness (calculated as a difference between the unit-cell parameter, $a = 1.155d_{100}$, and the pore diameter) for the methyl-functionalized silicas was somewhat larger (1.1–1.3 nm, see Table 1) than that expected for MCM-41 silicas with similar unit-cell size and pore volume.[46] This is consistent with a pore wall structure that features a silica backbone and a lining of organic groups, the latter having density much lower than that of silica. The specific surface area, pore diameter and primary pore volume were largely unchanged as the loading increased from 43% to 50%, but in the latter case, a marked increase in the external surface area and secondary pore volume was noted. To investigate whether this behavior may be indicative of separation into organosilica-rich and silica-rich phases, 100% methyl-functionalized sample was synthesized using pure TEMS. This material still exhibited high BET specific surface area (only 20–25% lower than that for the lower-loading materials under study), as expected from earlier studies,[47] and its porosity was mainly comprised of large mesopores, which is in accord with the amorphous nature of this material as suggested by XRD. The adsorption isotherm for this pure methylsilica material featured a prominent adsorption–desorption hysteresis loop (see Fig. 11), whereas some evidence of a similar hysteresis loop behavior was also observed for the

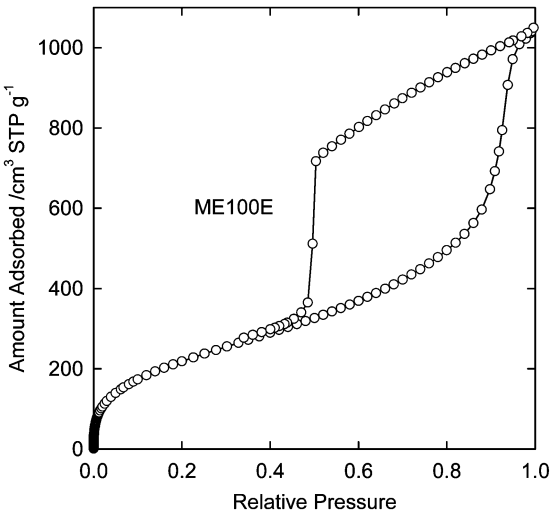

Fig. 11 Nitrogen adsorption isotherm for a methyl-functionalized silica synthesized from pure TEMS.

samples with lower loadings. On the basis of these observations, it appears likely that the extensive external surface area observed for the methyl-functionalized sample with 33–50% loading, and with 50% loading in particular, is related to some degree of separation into two high-surface-area phases, one being ordered and silica-rich, and the other being disordered and organosilica-rich.

The low-pressure relative adsorption of the solvent-extracted samples systematically decreased as the loading of methyl-functionalized precursor in the synthesis gel increased (Fig. 12), which is similar to the behavior observed for vinyl-functionalized materials with comparable loadings[21] and indicative of the increase in the surface concentration of methyl groups as the loading increased.[45]

The synthesis of silica with 50% methyl group loading was fairly reproducible. The nitrogen adsorption isotherm of a sample from the repeated synthesis was similar to that for the sample synthesized earlier (Fig. 13), although the adsorption capacity for the former was somewhat lower. As shown in Fig. 13, samples with similar adsorption properties are obtained independently of the method of the surfactant removal (solvent-extraction and calcination at 623 K were employed). The increase in outgassing temperature from 413 to

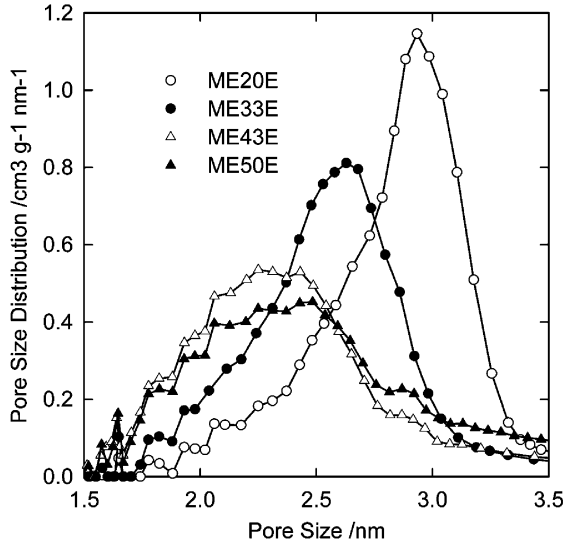

Fig. 10 Pore size distributions for methyl-functionalized silicas with 20–50% loadings of methyl groups.

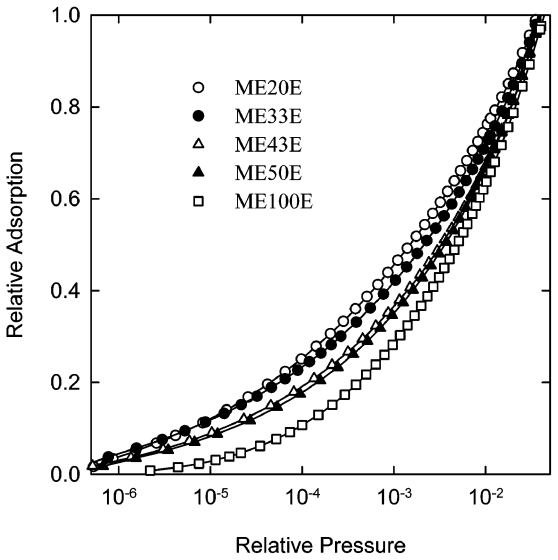

Fig. 12 Relative adsorption curves (amounts adsorbed divided by the BET monolayer capacity) for methyl-functionalized silicas.

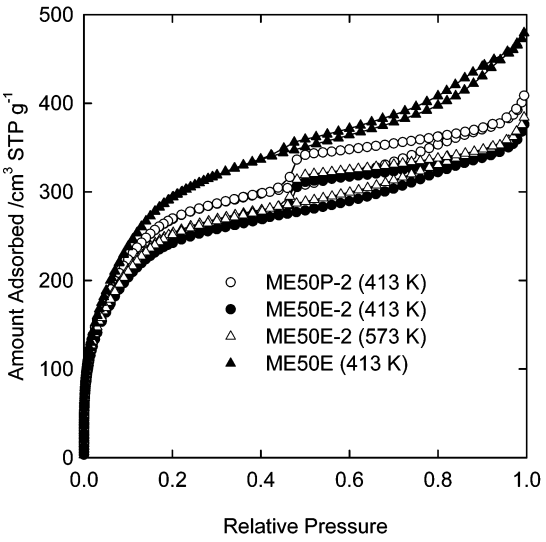

Fig. 13 Comparison of nitrogen adsorption isotherms for a methyl-functionalized silica with 50% loading of methyl groups with surfactant removed either *via* solvent-extraction or calcination. The outgassing temperature is denoted in parentheses. The isotherm for a sample from a different batch (ME50E, whose isotherm is shown in Fig. 8) is included to facilitate the comparison.

573 K did not lead to any appreciable changes in adsorption properties of the solvent-extracted sample, although this outgassing temperature was found to be sufficient to decompose most of the residual surfactant left after extraction. In the case of methyl-functionalized samples with lower organic group loadings, the reproducibility of the synthesis was not so good. Some samples shrunk appreciably or appeared to collapse partially upon solvent extraction. This is in contrast with the excellent reproducibility of the synthesis of vinyl-functionalized silicas under the same conditions.[22]

Conclusions

Silicas with high loadings of pendent methyl groups can be prepared *via* cocondensation of TEOS and TEMS under basic conditions using CTAB as a structure-directing agent. A nearly quantitative incorporation of the organosilane precursor was achieved for the loading as high as 50%. However, there is evidence of some separation into disordered organosilica-rich and ordered silica-rich phases for loadings of 33% and higher, which is particularly pronounced for the 50% loading. This phase separation manifests itself in the development of a prominent secondary porosity, but does not lead to any significant diminution of the BET specific surface area. This is possible because even a disordered organosilica synthesized from pure organosilica precursor under similar conditions exhibited a surface area only about 25% smaller than the ordered methyl-functionalized silicas. These results are in contrast to those for vinyl-functionalized silicas synthesized under the same conditions, in which case much higher loadings (up to about 65%) could be achieved without phase separation, and a prominent surface area drop was observed for higher loadings. Furthermore, the methyl groups were found to be much more thermally stable than vinyl groups, which offered an opportunity of template removal *via* calcinations in the former case.

Acknowledgements

M. J. acknowledges support by NSF Grant CHE-0093707. G. A. O. is Government of Canada Research Chair in Materials Chemistry. He acknowledges the Natural Sciences and Engineering Council of Canada (NSERC) for financial support.

References

1 J. S. Beck, J. C. Vartuli, W. J. Roth, M. E. Leonowicz, C. T. Kresge, K. D. Schmitt, C. T.-W. Chu, D. H. Olson, E. W. Sheppard, S. B. McCullen, J. B. Higgins and J. L. Schlenker, *J. Am. Chem. Soc.*, 1992, **114**, 10834.
2 T. Yanagisawa, T. Shimizu and K. Kuroda, *Bull. Chem. Soc. Jpn.*, 1990, **63**, 988.
3 A. Stein, B. J. Melde and R. C. Schroden, *Adv. Mater.*, 2000, **12**, 147.
4 A. Sayari and S. Hamoudi, *Chem. Mater.*, 2001, **13**, 3151.
5 T. Yanagisawa, T. Shimizu, K. Kuroda and C. Kato, *Bull. Chem. Soc. Jpn.*, 1990, **63**, 1535.
6 S. L. Burkett, S. D. Sims and S. Mann, *Chem. Commun.*, 1996, 1367.
7 D. J. Macquarrie, *Chem. Commun.*, 1996, 1961.
8 S. Inagaki, S. Guan, Y. Fukushima, T. Ohsuna and O. Terasaki, *J. Am. Chem. Soc.*, 1999, **121**, 9611.
9 B. J. Melde, B. T. Holland, C. F. Blanford and A. Stein, *Chem. Mater.*, 1999, **11**, 3302.
10 T. Asefa, M. J. MacLachlan, N. Coombs and G. A. Ozin, *Nature*, 1999, **402**, 867.
11 T. Asefa, M. J. MacLachlan, H. Grondey, N. Coombs and G. A. Ozin, *Angew. Chem. Int. Ed.*, 2000, **39**, 1808.
12 T. Asefa, M. Kruk, M. J. MacLachlan, N. Coombs, H. Grondey, M. Jaroniec and G. A. Ozin, *J. Am. Chem. Soc.*, 2001, **123**, 8520.
13 M. C. Burleigh, S. Dai, E. W. Hageman and J. S. Lin, *Chem. Mater.*, 2001, **13**, 2537.
14 X. Feng, G. E. Fryxell, L.-Q. Wang, A. Y. Kim, J. Liu and K. M. Kemner, *Science*, 1997, **276**, 923.
15 T. S. Zemanian, G. E. Fryxell, J. Liu, S. Mattigod, J. A. Franz and Z. Nie, *Langmuir*, 2001, **17**, 8172.
16 J. C. Vartuli, K. D. Schmidt, C. T. Kresge, W. J. Roth, M. E. Leonowicz, S. McCullen, S. D. Hellring, J. S. Beck, J. L. Schlenker, D. H. Olson and E. W. Sheppard, *Chem. Mater.*, 1994, **6**, 2317.
17 V. Antochshuk and M. Jaroniec, *Chem. Commun.*, 1999, 2373.
18 H.-P. Lin, L.-Y. Yang, C.-Y. Mou, S.-B. Liu and H.-K. Lee, *New J. Chem.*, 2000, **24**, 253.
19 D. J. Macquarrie, *Green Chem.*, 1999, 195.
20 Y. Mori and T. J. Pinnavaia, *Chem. Mater.*, 2001, **13**, 2173.
21 M. Kruk, T. Asefa, M. Jaroniec and G. A. Ozin, *J. Am. Chem. Soc.*, 2002, **124**, 6383.
22 M. Kruk, T. Asefa, M. Jaroniec and G. A. Ozin, *Stud. Surf. Sci. Catal.*, 2002, **141**, 197.
23 A. Corma, J. L. Jorda, M. T. Navarro and F. Rey, *Chem. Commun.*, 1998, 1899.
24 M. Koya and H. Nakajima, *Stud. Surf. Sci. Catal.*, 1998, **117**, 243.
25 A. Bhaumik and T. Tatsumi, *J. Catal.*, 2000, **189**, 31.
26 I. Diaz, C. Marquez-Alvarez, F. Mohino, J. Perez-Pariente and E. Sastre, *J. Catal.*, 2000, **193**, 283.
27 I. Diaz, C. Marquez-Alvarez, F. Mohino, J. Perez-Pariente and E. Sastre, *J. Catal.*, 2000, **193**, 295.
28 A. Bhaumik and T. Tatsumi, *Catal. Lett.*, 2000, **66**, 181.
29 N. Igarashi, Y. Tanaka, S.-I. Nakata and T. Tatsumi, *Chem. Lett.*, 1999, 1.
30 J. Joo, T. Hyeon and J. Hyeon-Lee, *Chem. Commun.*, 2000, 1487.
31 F. Babonneau, L. Leite and S. Fontlupt, *J. Mater. Chem.*, 1999, **9**, 175.
32 Y. J. Gong, Z. H. Li, D. Wu, Y. H. Sun, F. Deng, Q. Lou and Y. Yue, *Microporous Mesoporous Mater.*, 2001, **49**, 95.
33 C. E. Fowler, S. L. Burkett and S. Mann, *Chem. Commun.*, 1997, 1769.
34 D. J. Macquarrie, D. B. Jackson, S. Tailland, K. Wilson and J. H. Clark, *Stud. Surf. Sci. Catal.*, 2000, **129**, 275.
35 K. Moller, T. Bein and R. X. Fischer, *Chem. Mater.*, 1999, **11**, 665.
36 V. Goletto, M. Imperor and F. Babonneau, *Stud. Surf. Sci. Catal.*, 2000, **129**, 287.
37 K. Wilson, A. F. Lee, D. J. Macquarrie and J. H. Clark, *Appl. Catal., A*, 2002, **228**, 127.
38 J. A. Elings, R. Ait-Meddour, J. H. Clark and D. J. Macquarrie, *Chem. Commun.*, 1998, 2707.
39 M. H. Lim, C. F. Blanford and A. Stein, *Chem. Mater.*, 1998, **10**, 467.
40 K. S. W. Sing, D. H. Everett, R. A. W. Haul, L. Moscou, R. A. Pierotti, J. Rouquerol and T. Siemieniewska, *Pure Appl. Chem.*, 1985, **57**, 603.
41 R. Ryoo, I.-S. Park, S. Jun, C. W. Lee, M. Kruk and M. Jaroniec, *J. Am. Chem. Soc.*, 2001, **123**, 1650.
42 M. Jaroniec, M. Kruk and J. P. Olivier, *Langmuir*, 1999, **15**, 5410.
43 E. P. Barrett, L. G. Joyner and P. P. Halenda, *J. Am. Chem. Soc.*, 1951, **73**, 373.
44 M. Kruk, M. Jaroniec and A. Sayari, *Langmuir*, 1997, **13**, 6267.
45 M. Kruk and M. Jaroniec, *Chem. Mater.*, 2001, **13**, 3169.
46 M. Kruk, M. Jaroniec and A. Sayari, *Chem. Mater.*, 1999, **11**, 492.
47 D. A. Loy, B. M. Baugher, C. Baugher, D. A. Schneider and K. Rahimian, *Chem. Mater.*, 2000, **12**, 3624.